Calculated geometry and paramagnetic hyperfine structure of the Cu_7 cluster

Ramiro Arratia-Pérez [a,*], Luis Alvarez-Thon [a], Patricio Fuentealba [b]

[a] *Departamento de Ciencias Químicas, Facultad de Ecología y Recursos Naturales, Universidad Andrés Bello, República 275, Santiago, Chile*
[b] *Departamento de Física, Facultad de Ciencias, Universidad de Chile, Casilla 653, Santiago, Chile*

Abstract

All-electron spin polarized DFT calculations have been performed to optimize the pentagonal bipyramidal (D_{5h}) geometry of the Cu_7 cluster by using the B3LYP and the B3PW1 functionals with different basis sets. Dirac scattered-wave and its non-relativistic limit calculations are used to calculate the ^{63}Cu hyperfine coupling constants using a first order perturbational procedure. Our calculations for the Cu_7 cluster predict the $^2A_2''$ as its ground state. The calculated hyperfine coupling constants are in reasonable agreement with those experimentally determined for Cu_7 in a matrix isolated ESR study by Van Zee and Weltner

1. Introduction

The Cu_7 cluster has been the subject of experimental and recent theoretical studies [1–4]. Howard et al. [1] observed the ESR spectrum of a copper cluster in a deuterated cyclohexane matrix that was attributed to the Cu_5 cluster, but later reinterpreted it as due to the Cu_7 cluster [2]. The same spectrum in neon matrices was observed and analyzed by Van Zee and Weltner [3], who postulated a pentagonal bipyramidal (D_{5h}) structure for Cu_7. Recent nonrelativistic (NR) DFT calculations [4] using the B3PW91 [5,6] functional and the LANL2DZ basis set for effective core potentials for copper atoms [7,8], calculated the pentagonal bipyramidal (D_{5h}) structure to be of the lowest energy.

It is recognized that electron spin resonance (ESR) spectroscopy applied to the study of metal clusters has been useful in elucidating cluster geometries, electronic states and spin distributions [9–16]. In particular, the overall ESR spectrum of Cu_7 shows 16 groups of lines in which only 14 are distinguishable, which are produced by the hyperfine interaction (hfi) of the unpaired electron spin with two equivalent ^{63}Cu nuclei, and each of these lines are then split by the hfi with five equivalent ring atoms [3]. Because of some uncertainties in the assignment of these 16 lines in each group, the 'most probable centers' were selected on the basis of the 14 observed lines that were needed for calculating the isotropic and dipolar magnetic parameters (A_{iso} and A_{dip}), along with estimating the approximate s and p densities which were derived, as usual, by comparisons with atomic data [10,11]. We reexamine these approximations because the estimated s and p densities may vary, mainly due to cluster bonding and/or orbital hybridization effects.

In this study, we report the results of all-electron DFT calculations for geometry optimization using the B3PW91 [5,6] and the B3LYP [6,17,18] functionals with different basis sets, and, the results of the calculations of the hyperfine coupling constants of the Cu_7 cluster using self-consistent Dirac scattered wave (DSW) functions as

* Corresponding author. Fax: +562 661 8269.
E-mail address: rarratia@unab.cl (R. Arratia-Pérez).

the starting point. Since the DSW wave functions include spin–orbit effects (and transform according to the D_{5h} double point group), only the external magnetic field and the nuclear hfi need be included in the relativistic first-order perturbation scheme [9,10,21,22].

2. Methods and detail of the calculations

All electron spin-polarized DFT calculations have been performed using two different hybrid functionals (B3LYP and B3PW91) to optimize the D_{5h} geometry of Cu_7 using the two different basis sets 6-31G* and the 6-311 + G*. An extra very tight contracted s-function was added to calculate the ESR properties [19]. The different types of calculations reported here are named as B3LYP/6-31G* (DFT-I), B3LYP/6-311 + G* (DFT-II), B3PW91/6-311 + G* (DFT-III) and B3LYP/6-311 + G* plus tight s-function (DFT-IV), respectively. All these calculations were performed using the GAUSSIAN 98 package [20].

The spin-restricted self-consistent-field Dirac scattered-wave (SCF-DSW) method was developed by Yang, Case, and Arratia-Pérez [21–28]. This method employs the molecular Dirac equation to generate the one-electron cluster orbitals, and thus implicitly includes the principal non-quantum electrodynamical relativistic effects (mass-velocity, Darwin and spin–orbit) at the SCF stage. In this formalism, an effective Coulomb and exchange-correlation potential approximate the cluster wave function as a Slater determinant of one-electron 4-component molecular spinor (MS) [29]. For the exchange-correlation potential we used a local density potential [30] relativistically modified according to MacDonald and Vosko [31–33]. The various DSW calculations are also designated accordingly to the different optimized geometries obtained by the DFT calculations named above, see Table 1.

Once the Dirac self-consistent cluster wave function Φ is obtained, we proceed throughout a first-order perturbation procedure by considering the effects of external magnetic fields being described by a relativistic perturbation Hamiltonian $H_D = e\boldsymbol{\alpha}\cdot\mathbf{A}$, where $\boldsymbol{\alpha}$ is the 4×4 Dirac matrix composed of zeros on the diagonal, and the Pauli spin matrices in the off-diagonal positions, and, $\mathbf{A}$ is the electromagnetic vector potential. In the presence of nuclear magnetic dipole moments $\boldsymbol{\mu} = g_N\beta_N\mathbf{I}$, the electromagnetic vector potential $\mathbf{A}$ is represented by $\mathbf{A} = (\boldsymbol{\mu}\times\mathbf{r})/r^3$. Thus, the magnetic hfi are described by the Dirac perturbation Hamiltonian $H_D = e\boldsymbol{\alpha}\cdot[(\boldsymbol{\mu}\times\mathbf{r})/r^3]$ Therefore, the $\langle\Phi|H_D|\Phi\rangle$ matrix elements of these magnetic operators are evaluated in the basis spanning the rows 1 and 2 (designated hereafter as the bras $|1\rangle$ and $|2\rangle$) of the double valued irreducible representations of the cluster orbital occupying the single electron spin. Since the $\boldsymbol{\alpha}$ matrices are off-diagonal, the evaluation of the matrix elements involve products of the 'large' and 'small' components of the Dirac cluster wave function. Therefore, both the large and small components of the relativistic wave function carry information related to molecular magnetic behavior [9,22,26–28].

The resulting perturbation energies are fitted to the usual spin Hamiltonian $H_{spin} = \mathbf{I}_n\cdot\mathbf{A}_{hfi}\cdot\mathbf{S}$, where a convenient parametrized value of $\mathbf{S} = 1/2$ is used to describe the ground state Kramers doublet. $\mathbf{I}_n$ is a nuclear spin operator, n denotes the ^{63}Cu(2) and ^{63}Cu(5) nuclei, and $\mathbf{A}_{hfi}$ is its associated magnetic hyperfine tensors [9,26–28]. Thus, H_{spin} is evaluated over the electron spin functions in a basis for which S_Z is diagonal. In order to compare matrix elements, the molecular Dirac spinors are rotated so that the z-component of H_D is also diagonal, i.e., the H_D operator is diagonal when the external field is parallel to this axis. After such a rotation, the matrix elements of H_D may be directly identified with those of H_{spin}, i.e.,

$$\begin{aligned}\mathbf{A}_{ix} &= 2\beta_e g_N\beta_N \mathrm{Re}\,\langle 1|(\mathbf{r}\times\boldsymbol{\alpha})_i/r^3|2\rangle,\\ \mathbf{A}_{iy} &= 2\beta_e g_N\beta_N \mathrm{Im}\,\langle 1|(\mathbf{r}\times\boldsymbol{\alpha})_i/r^3|2\rangle, \quad i = x,y,z\\ \mathbf{A}_{iz} &= 2\beta_e g_N\beta_N\langle 1\mid(\mathbf{r}\times\boldsymbol{\alpha})_i/r^3|1\rangle,\end{aligned} \tag{1}$$

the calculated hyperfine tensors (A_{hfi}) include all the Fermi contact or isotropic, spin-dipolar, and orbital contributions due to spin–orbit effects. For the cluster considered here, the magnetic tensors are diagonal in the molecular frame, with $A_{XX} = A_{YY} = A_\perp$ and $A_{ZZ} = A_\parallel$. Its must be noted that there is no need to use different operators to represent these contributions, as required in conventional nonrelativistic theories [10,14].

Table 1
Geometry optimization by all-electron spin polarized DFT calculations[a]

DFT calculations[b]	I	II	III
Functional	B3LYP	B3LYP	B3PW91
Basis set	6-31G*	6-311 + G*	6-311 + G*
d(Cu(5)–Cu(5)) (Å)	2.265	2.502	2.478
d(Cu(2)–Cu(5)) (Å)	2.265	2.484	2.456
Ground state	$^2A_2''$	$^2A_2''$	$^2A_2''$

[a] Cu(5) denotes the ring atoms, while Cu(2) denotes the axial atoms.
[b] B3PW91/LANL2DZ calculation predicts both distances equal to 2.500 Å. See [4].

3. Results and discussion

In Table 1, the optimized Cu(5)–Cu(5) and Cu(2)–Cu(5) distances are displayed. One can see that the Cu(5)–Cu(5) distances obtained by using the 6-311 + G* basis set are marginally larger by about 0.02 Å than the Cu(2)–Cu(5) distances when one uses the B3LYP or the B3PW91 functional. Whereas the dis-

tances obtained by using the smaller 6-31G* basis set are shorter and equal, the DFT-B3PW91/LANL2DZ calculation gives the same bond length for both distances [4].

The calculated spin densities for the $^2A_2''$ ground state of Cu_7 are listed in Table 2. It can be seen from this table that all the calculations show that most of the electron spin distribution reside on axial nuclei, and this compares well with the empirical estimate of about 29% [3]. It should be noted, however, that the ρ_s empirical estimate was calculated as the ratio of A_{iso}(cluster) to that of the free atom, by taking into account only the sσ character and neglecting the p and d contributions [3]. Also, it can be noted from Table 2, that the calculated electron spin distribution from the ring nuclei are all positive, while the empirical estimate is ambiguous. Furthermore, we can verify that for a unit spin population all the calculations reported here obey $2\rho(2) + 5(5) = 1.000$, as it should be, while the empirical estimate does not.

In relativistic electron theory the spin distributions arising from $j = 1/2$ states are spherically symmetric, and its contributions to the magnetic interactions are isotropic. The spin distributions arising from $j = 3/2$ and 5/2 states, however give rise to anisotropic magnetic interactions since these are nonspherical contributions [22,26–28]. Applying these concepts, we estimated the relativistic isotropic ρ_{iso} and anisotropic ρ_{aniso} spin populations for each magnetic nuclei of the Cu_7 cluster. Thus, for each ^{63}Cu(2) and ^{63}Cu(5) nuclei of Cu_7 we obtained that most of the electron spin distribution is isotropic and resides (~24%) on each axial nuclei and about 3% on each ring nuclei. The rest of the electron spin distribution is anisotropic and distributed on the axial (~4%) and ring (~8%) nuclei. In Fig. 1 we depict the relativistic spin density, where it can be seen that most of the electron spin distribution resides on the axial nuclei.

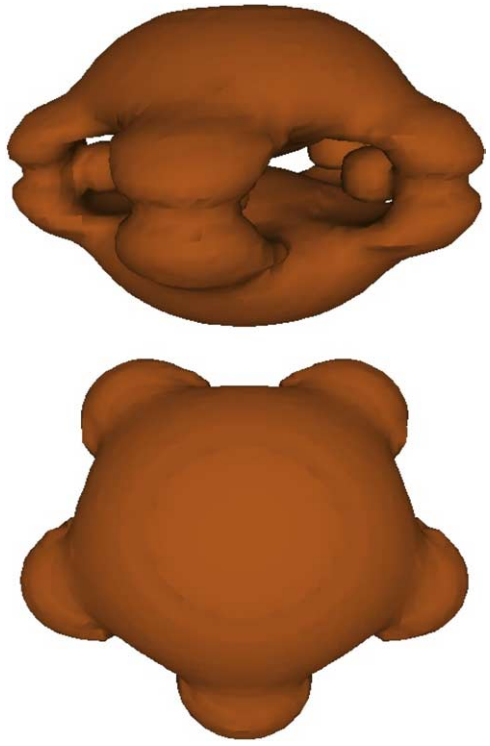

Fig. 1. Relativistic spin density three-dimensional (3D) orbital plot (electron/bohr^3)^3 of the $^2A_2''$ ground state of Cu_7. The isosurface range is between 0.05 and 0.15.

Table 2
Spin densities for the $^2A_2''$ ground state of Cu_7[a]

Calculation	$\rho(2)$	$\rho(5)$
DFT-I	0.218	0.113
DSW-NR-I[b]	0.270	0.092
DSW-I[c]	0.265	0.094
DFT-II	0.345	0.062
DSW-NR-II	0.282	0.087
DSW-II	0.275	0.090
DFT-III	0.406	0.037
DSW-NR-III	0.280	0.088
DSW-III	0.275	0.090
DFT-IV[d]	0.345	0.062
Empirical[e]	0.291	±0.009

[a] For a unit spin population these calculations obey $2\rho(2) + 5\rho(5) = 1.000$, while the empirical analysis does not.

[b] DSW-NR: non-relativistic calculation by setting the speed of light to a very large value ($c = \infty$) into the relativistic (DSW) code.

[c] DSW: fully relativistic (Dirac) calculations.

[d] Is a DFT-B3LYP/6-311 + G* + s-tight function calculation.

[e] spin densities for s-electrons estimated as the ratio of A_{iso} (i) to that of A_{iso} (free atom), see [3].

The calculated magnetic resonance parameters for both clusters are given in Table 3. It can be seen that the DFT calculated A_{iso} parameters for the axial nuclei are in close agreement with the empirical estimate, except the small basis set calculation (DFT-I), indicating that for calculating this magnetic parameter larger basis sets are required. Interestingly, the calculated A_{iso} parameters for the ring nuclei are negative, indicating that this arises due to spin polarization effects, since the g_N value for copper nuclei is positive [10,11]. The calculated A_{iso} results are in contrast with the empirical estimate of a positive A_{iso} parameter, but the empirical estimated value has approximately the same magnitude as the calculated values.

The calculated and experimental hyperfine coupling constants are also given in Table 3. The calculated values are obtained using the relativistic SCF-DSW and DSW-NR calculations. It can be seen from this table, that the calculated and experimental values for the axial ^{63}Cu nuclei agree in the sense that $A_\perp > A_\parallel$,. and, the calculated and experimental values for the ^{63}Cu ring nuclei agree in the sense that both components of the hyperfine coupling constants are isotropic since $A_\perp = A_\parallel$ indicating that the experimental assumption is correct [3].

Table 3
Paramagnetic parameters for the $^{63}Cu_7$ cluster in its $^2A_2''$ Kramers ground state[a,b]

Parameters	Calculations	^{63}Cu(2)	^{63}Cu(5)
A_{iso}[c]	DFT-I	1195	−21
	DFT-II	1806	−43
	DFT-III	1747	−73
	DFT-IV	1787	−53
	Empirical	1747	54[d]
$A_\perp$	DSW-NR-I	1839	40
	DSW-I	1949	42
	DSW-NR-II	1928	33
	DSW-II	2068	37
	DSW-NR-III	1920	34
	DSW-III	2060	38
	Experimental[b,d]	1794	54[d]
$A_\parallel$	DSW-NR-I	1783	40
	DSW-I	1892	42
	DSW-NR-II	1887	33
	DSW-II	2015	37
	DSW-NR-III	1868	34
	DSW-III	2006	38
	Experimental[b,d]	1654	54[d]

[a] All values in MHz.
[b] ESR spectrum in a Ne matrix, see [3].
[c] Calculated DFT values of $(8\pi/3)g_e\beta_e g_N\beta_N|\phi_{\alpha,\beta}(0)|^2$.
[d] Assumed value for $A_\perp(5) = A_\parallel(5) = A_{iso}(5)$, see [3].

Relativistic effects on the electronic structure and magnetic properties of this copper cluster are not very significant. Moreover, the hyperfine coupling constants calculated with the non-relativistic (DSW-NR) calculations are closer to the experimental values. This conclusion can also be inferred from the experimental $\Delta g_\perp = 0.069$ and $\Delta g_\parallel = 0.000$ parameters, since they show small deviations from the spin-only value.

4. Conclusions

Thus, we can conclude that the unpaired electron spin in Cu_7 spend most of its time on each axial ^{63}Cu(2) nucleus, and that our spin distribution, geometry optimization, and magnetic hyperfine coupling constants calculations, are in reasonable accord with the ESR spectral identification of Cu_7 as pentagonal bipyramidal.

Acknowledgements

We gratefully acknowledge the support of the Grants UNAB-DI-10-02, Fondecyt 1030148, Fondecyt 1010649 and the Millennium Nucleus for Applied Quantum Mechanics and Computational Chemistry, P02-004-F.

References

[1] J.A. Howard, R. Sutcliffe, J.T. Tse, B. Mile, Chem. Phys. Lett. 94 (1983) 561.
[2] J.A. Howard, B. Mile, Electron Spin Resonance (Specialist Periodical Reports, vol. 11B, London, 1988).
[3] R.J. Van Zee, W. Weltner Jr., J. Chem. Phys. 92 (1990) 6976.
[4] P. Jaque, A. Toro-Labbé, J. Chem. Phys. 117 (2002) 3208.
[5] J.P. Perdew, W.R. Wang, Phys. Rev. B 45 (1992) 13244.
[6] A.D. Becke, J. Chem. Phys. 98 (1993) 5648.
[7] P.J. Hay, W.R. Wadt, J. Chem. Phys. 82 (1985) 270.
[8] P.J. Hay, W.R. Wadt, J. Chem. Phys 82 (1985) 284.
[9] J.E. Harriman, Theoretical Foundations of Electron Spin Resonance, Academic, New York, 1978.
[10] W. Weltner Jr., Magnetic Atoms and Molecules, Dover, New York, 1989.
[11] J.R. Morton, K.F. Preston, J. Magn. Reson. 30 (1978) 577.
[12] J.A. Howard, K.F. Preston, B. Mile, J. Am. Chem. Soc. 103 (1981) 6226.
[13] J.H.B. Chenier, C.A. Hampson, J.A. Howard, B. Mile, J. Phys. Chem. 93 (1989) 114.
[14] K. Kernisant, G.A. Thompson, D.M. Lindsay, J. Chem. Phys. 82 (1985) 4739.
[15] A. van der Pool, E.J. Reijserse, E. de Boer, Mol. Phys. 75 (1992) 37.
[16] J. Michalik, T. Wasowicz, A. van der Pool, E.J. Reijerse, E. de Boer, J. Chem. Soc. Chem. Commun. (1992) 29.
[17] C. Lee, W. Yang, R.G. Parr, Phys. Rev. B 37 (1988) 785.
[18] B. Miehlich, A. Savin, H. Stoll, H. Preuss, Chem. Phys. Lett. 157 (1989) 200.
[19] V. Barone, R. Fournier, F. Mele, N. Russo, C. Adamo, Chem. Phys. Lett. 237 (1995) 189.
[20] M.J. Frisch et al., Gaussian 98, Revision A.9, Gaussian, Inc., Pittsburgh PA, 1998.
[21] C.Y. Yang, D.A. Case, in: J.P. Dahl, J. Avery (Eds.), Local Density Approximations in Quantum Chemistry and Solid State Physics, Plenum, New York, 1983.
[22] R. Arratia-Pérez, D.A. Case, J. Chem. Phys. 79 (1983) 4939.
[23] R. Arratia-Pérez, L. Hernández-Acevedo, J. Chem. Phys. 109 (1998) 3497.
[24] R. Arratia-Pérez, L. Hernández-Acevedo, J. Chem. Phys. 110 (1999) 2529.
[25] R. Arratia-Pérez, L. Hernández-Acevedo, J. Chem. Phys. 111 (1999) 168.
[26] R. Arratia-Pérez, L. Hernández-Acevedo, J. Chem. Phys. 118 (2003) 7425.
[27] R. Arratia-Pérez, L. Hernández-Acevedo, L. Alvarez-Thon, J. Chem. Phys. 108 (1998) 5795.
[28] L. Alvarez-Thon., L. Hernández-Acevedo, R. Arratia-Pérez, J. Chem. Phys. 115 (2001) 726.
[29] G.L. Malli, J. Oreg, J. Chem. Phys. 63 (1975) 831.
[30] L. Hedin, B.I. Lundqvist, J. Phys. C 4 (1974) 2064.
[31] H. MacDonald, S.H. Vosko, J. Phys. C 12 (1979) 2977.
[32] A.K. Rajagopal, J. Phys. C 11 (1978) L943.
[33] A.K. Rajagopal, Adv. Chem. Phys. 41 (1980) 59.